Atmospheric nonequilibrium mini-plasma jet created by a 3D printer

Takamatsu, Toshihiro

Kawano, Hiroaki

Miyahara, Hidekazu

Azuma, Takeshi

Okino, Akitoshi

(Citation)
AIP Advances,5(7):077184-077184

(Issue Date)
2015-07

(Resource Type)
journal article

(Version)
Version of Record

Atmospheric nonequilibrium mini-plasma jet created by a 3D printer

Toshihiro Takamatsu, Hiroaki Kawano, Hidekazu Miyahara, Takeshi Azuma, and Akitoshi Okino

Citation: AIP Advances **5**, 077184 (2015); doi: 10.1063/1.4928034
View online: http://dx.doi.org/10.1063/1.4928034
View Table of Contents: http://scitation.aip.org/content/aip/journal/adva/5/7?ver=pdfcov
Published by the AIP Publishing

AIP ADVANCES **5**, 077184 (2015)

Atmospheric nonequilibrium mini-plasma jet created by a 3D printer

Toshihiro Takamatsu,[1,2,a] Hiroaki Kawano,[2] Hidekazu Miyahara,[2] Takeshi Azuma,[1] and Akitoshi Okino[2]
[1]*Kobe University Graduate School of Medicine, Department of Gastroenterology, 7-5-1 Kusunoki-cho, Chuo-ku, Kobe, 650-0017, Japan*
[2]*Tokyo Institute of Technology, Department of Energy Sciences, J2-32, 4259 Nagatsuta, Midori-ku, Yokohama, 226-8502, Japan*

(Received 29 June 2015; accepted 22 July 2015; published online 31 July 2015)

In this study, a small-sized plasma jet source with a 3.7 mm head diameter was created via a 3D printer. The jet's emission properties and OH radical concentrations (generated by argon, helium, and nitrogen plasmas) were investigated using optical emission spectrometry (OES) and electron spin resonance (ESR). As such, for OES, each individual gas plasma propagates emission lines that derive from gases and ambient air inserted into the measurement system. For the case of ESR, a spin adduct of the OH radical is typically observed for all gas plasma treatment scenarios with a 10 s treatment by helium plasma generating the largest amount of OH radicals at 110 μM. Therefore, it was confirmed that a plasma jet source made by a 3D printer can generate stable plasmas using each of the aforementioned three gases. [http://dx.doi.org/10.1063/1.4928034]

An atmospheric plasma source can generate high density plasma and enable a continuous plasma treatment state without the aid of a vacuum system. Therefore, such a source can provide high-efficiency and high-speed treatments, which are desired in various industrial fields, including surface treatment,[1] harmful gas decomposition,[2] toxic degradation,[3] and elemental analysis.[4–11] Recently, heat-sensitive materials such as living bodies can be effectively irradiated with plasma, since atmospheric nonequilibrium plasma can be generated from about room temperature to approximately 100°C using argon and helium gases. Using this plasma, the efficacies of bacterial inactivation,[12] blood coagulation,[13,14] wound healing,[15,16] and cancer cell eradication[17,18] were investigated. Therefore, various plasma sources have been developed for such potential applications, and they have ultimately attracted much attention in the medical field. Currently, most products have been fabricated by mechanical processing and welding. There are many marketplace needs for a reduction in the size of certain plasma sources to support more "refined" applications, but present mechanical processing technologies inherently have limitations as to the degree of downsizing, especially in regard to complicated shapes and unification of parts. In response to such needs, a microplasma source that can generate tiny plasma from a hole of less than 1 mm in diameter has been developed.[11] However, this plasma source has no aptitude for practical use in the realms of surface treatment or bacterial inactivation due to its power input limitations and high gas flow rate.

Thus, in an endeavor to fabricate a new miniature-sized plasma source that was exempt from the potential limitations discussed above, the use of a 3D printer was evaluated for effectiveness.[19,20] The designing of metal 3D printing by CAD is flexible with the inclusion of a detail curve and complicated channel, which conventional mechanical processing and welding technologies are unable to manufacture. In addition, selectable materials include resins as well as metals.[21] When considering all these factors, the use of a 3D printer may be deemed the most effective approach for reducing the size (and thus enhancing the applicabilities) of potential plasma sources. In this study,

[a]Author to whom correspondence should be addressed. Electronic mail: toshihiro@plasma.es.titech.ac.jp

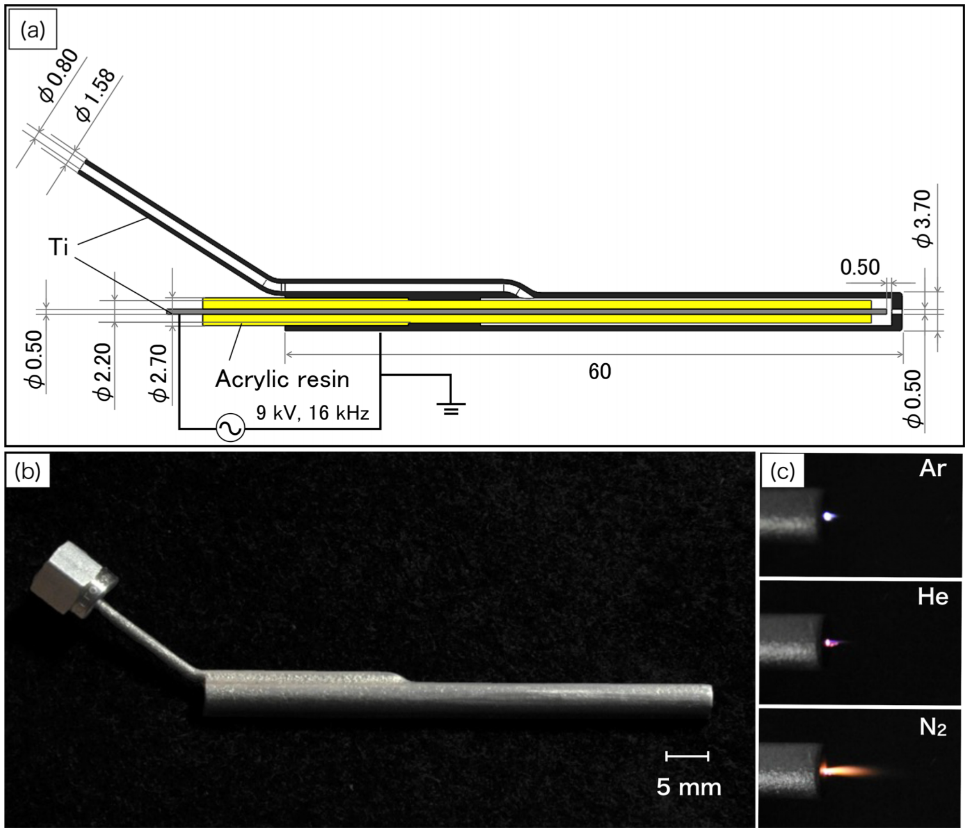

FIG. 1. Atmospheric plasma jet (a) cross-sectional view of plasma jet and scale, (b) plasma jet body, (c) produced plasma by argon, helium, and nitrogen gases.

an atmospheric nonequilibrium plasma jet source was created using a 3D printer, and the properties of generated plasmas were investigated.

The subject plasma source was constructed by a metal 3D(M280, Electro Optical Systems Inc.) and resin 3D (ProJet 3500 HD, 3D Systems Inc.) printers. The machining errors are approximately 0.125 and 0.05 mm, respectively. Figure 1(a) shows a cross-sectional view of the plasma jet and scale, and Fig. 1(b) shows a photograph of the plasma jet body made by the metal 3D printer. The body, which is 60 mm in length with a 3.7 mm head diameter, is grounded, and the interior high-voltage 0.5 mm electrode is connected to a power supply (Plasma Concept Tokyo, Inc.) with 16 kHz and 9 kV. The discharge gap, which is the distance between the high voltage and grounded electrodes, is fixed at 0.5 mm. The electrodes are composed of titanium and insulated by an acrylic resin. A segment of the gas insertion apparatus is unified with the printer body, and the gas being inserted through a tube of 1.58 mm o.d. and 0.8 mm i.d. Generated plasma flows out through a hole of 0.5 mm diameter at a flow rate of ≧0.3 L/min. As shown in Fig. 1(c), the plasma source can generate stable plasmas with argon, helium, and nitrogen gases. The plasmas are nonequilibrium, and the gas temperature of afterglow ranged from room temperature to approximately 100°C.

Spectrum analysis of plasma radiation is necessary to confirm the plasma generation. Argon, helium, and nitrogen plasma jets were generated at a flow rate of 0.3 L/min, and emission spectra were observed by spectroscope [Maya2000Pro (200–1100 nm); Ocean Optics, Inc.] under open-air conditions. An optical fiber was set at a distance of 10 mm from the plasma outlet, and a quartz plate (thickness of 1 mm) was strategically placed to prevent direct exposure to the fiber core.[1] Figure 2 shows the OES of the plasma jets that were created with the three different gases. Each of the argon, helium, and nitrogen plasmas had emission lines originating from their component species. In addition, the argon and helium plasmas had strong emissions of $OH(A^2\Sigma^+ - X^2\Pi_{3/2})$, and the helium plasma showed an atomic oxygen line originating from the ambient air. Thus, the reactions

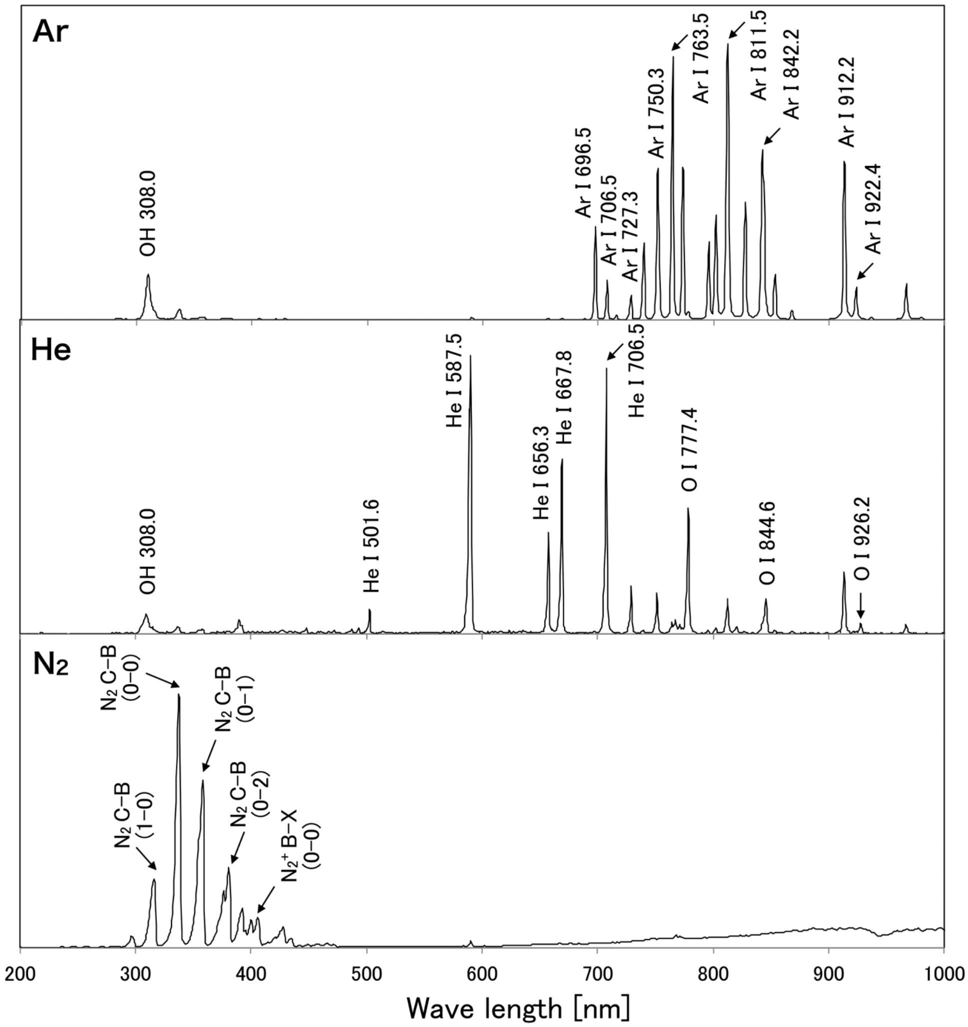

FIG. 2. Emission spectra of various gas plasmas. Observed gas species were argon, helium, and nitrogen gases.

relating to the individual gas species are shown below in Equations (1) to (6).

$$Ar + e \rightarrow Ar^* + e \qquad \text{(Ref. 22)} \tag{1}$$

$$He + e \rightarrow He^* + e \qquad \text{(Ref. 23)} \tag{2}$$

$$N_2 + e \rightarrow N_2(A\,^3\Sigma_u^+) + e \qquad \text{(Ref. 24)} \tag{3}$$

$$He^* + O_2 \rightarrow He + 2O \qquad \text{(Ref. 25)} \tag{4}$$

$$Ar^* + H_2O \rightarrow Ar + H\cdot + HO\cdot \qquad \text{(Ref. 22)} \tag{5}$$

$$He^* + H_2O \rightarrow He + H\cdot + HO\cdot \qquad \text{(Ref. 26)} \tag{6}$$

It is believed that each potential plasma treatment course (e.g., bacterial inactivation and blood coagulation) is ultimately sponsored by a reactive oxygen species and OH radical.[27] Therefore, the concentrations of OH radical, which are generated by the plasmas of argon, helium, and nitrogen, were investigated. The OH radical reacts with individual spin trapping agents, and the spin adducts can be identified using electron spin resonance (ESR) measurements. The spin trapping agent used in this study, 5,5-Dimethyl-1-pyrroline-N-oxide (DMPO), was effectively employed as the OH radical detector.[28] The agent was dissolved in a phosphate-buffered saline (-) (PBS(-)) solution, which had a pH of 7.5, and a fixed DMPO concentration of 200 mM.[29] Plasma treatments of 200 μL solutions were conducted at a 6 mm distance between the plasma source outlet and liquid surfaces

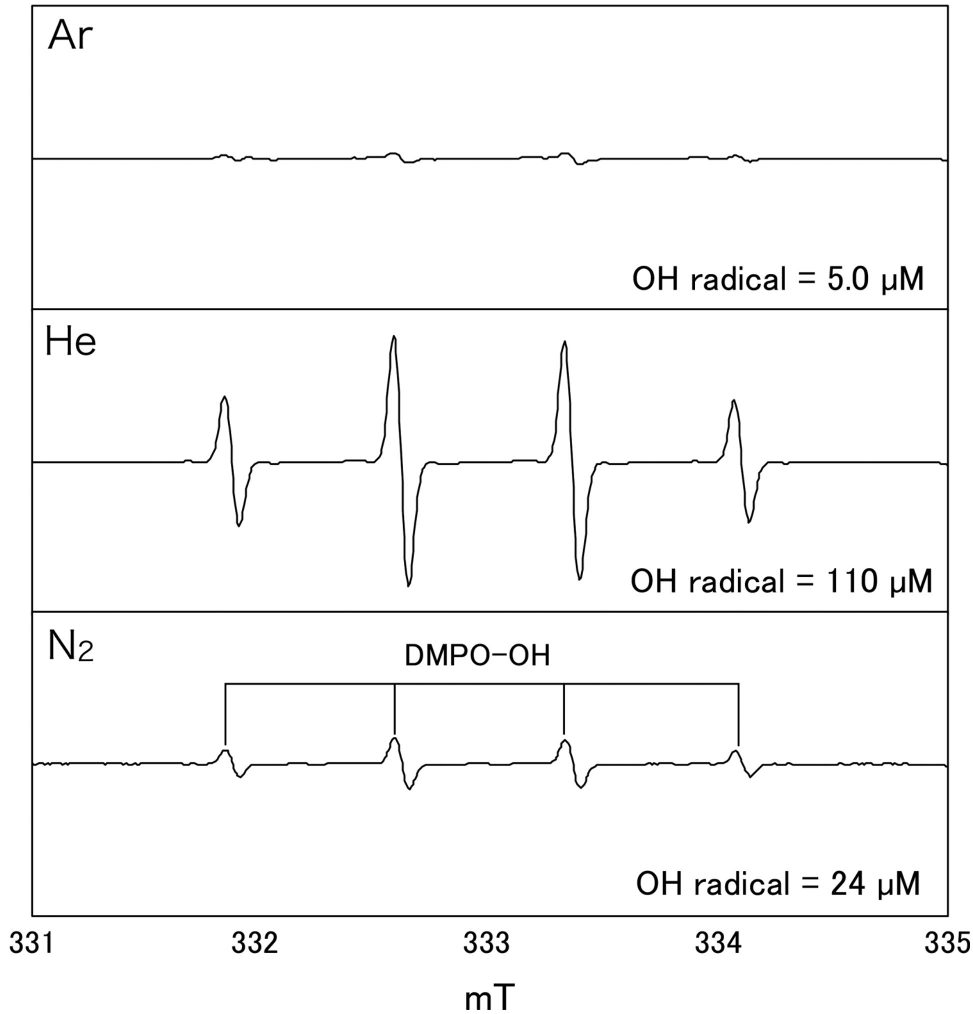

FIG. 3. ESR spectra of each gas plasma. Observed gas species were argon, helium, and nitrogen gases. As setup, 9.424818 GHz of microwave frequency, 2 min of sweep time, 100 kHz of modulation frequency, 335.5 ± 5 mT of magnetic field, 0.1 mT of modulation width, and 0.1 s of time constant were set.

with a flow rate of 0.3 L/min for 10 s. The amount of reactive species was calibrated with spin adducts of 2,2,6,6-tetramethylpiperidine 1-oxyl, which identified the amount of OH radical. Results showed that helium plasma generated the largest amounts of OH radical at 110 μM, as shown in Fig. 3. The amounts of OH radical generated by argon and nitrogen plasmas were estimated at 5.0 and 24 μM, respectively. In terms of using argon, helium, and nitrogen, which are all inert gases, the results suggest that liquid phase reactions were initiated and that the OH radical was generated via reacting within a gas–liquid interface, as depicted in Equations (5) to (7).

$$N_2\left(A\,{}^3\Sigma_u^+\right) + H_2O \rightarrow N_2 + H\cdot + HO\cdot \qquad \text{(Ref. 24)} \tag{7}$$

From this study, it was concluded that the endeavor to develop a miniature-sized plasma source using a 3D- printer was a success. Moreover, it was confirmed that this plasma source generates stable plasmas with argon, helium, and nitrogen gases. The plasma source can be attached to a temperature controlled unit,[30] which allows a user to easily control plasma gas temperatures. Therefore, this correlates to the notion that such plasma gases can be accurately controlled at around body temperature and that heat-sensitive targets can be effectively treated without thermal damage. As such, miniature-sized plasma source has the potential to be used as a medical device to render states of bacterial inactivation and blood coagulation under a narrow surgical field.

This study was supported by a Grant-in-Aid for Research Activity Start-up Grant Number 26886009 and a Grant-in-Aid for Challenging Exploratory Research Grant Number 26670382. The authors thank Plasma Concept Tokyo, Inc. for their support and collaboration.

[1] T. Takamatsu, H. Hirai, R. Sasaki, H. Miyahara, and A. Okino, IEEE Trans. Plasma Sci. **41**, 119 (2013).
[2] T. Tamura, Y. Kaburaki, R. Sasaki, H. Miyahara, and A Okino, IEEE Trans. Plasma Sci. **39**, 1684 (2011).
[3] T. Takamatsu, H. Miyahara, T. Azuma, and A. Okino, J. Toxicol. Sci. **39**, 281 (2014).
[4] K. Shigeta, G. Köllensperger, E. Rampler, H. Traub, L. Rottmann, U. Panne, A. Okino, and N. Jakubowski, J. Anal. At. Spectrom. **28**, 637 (2013).
[5] K. Shigeta, H. Traub, U. Panne, A. Okino, L. Rottmann, and N. Jakubowski, J. Anal. At. Spectrom. **28**, 646 (2013).
[6] T. Iwai, Y. Takahashi, H. Miyahara, and A. Okino, Anal. Sci. **29**, 1141 (2013).
[7] H. Miyahara, T. Iwai, Y. Nagata, Y. Takahashi, O. Fujita, Y. Toyoura, and A. Okino, J. Anal. At. Spectrom. **29**, 105 (2014).
[8] K. Shigeta, Y. Kaburaki, T. Iwai, H. Miyahara, and A. Okino, J. Anal. At. Spectrom. (2015), doi:10.1039/C3JA50382H.
[9] T. Iwai, K. Kakegawa, M. Aida, H. Nagashima, T. Nagoya, M. Kanamori-Kataoka, H. Miyahara, Y. Seto, and A. Okino, Anal. Chem. **87**, 5707 (2015).
[10] T. Iwai, K Shigeta, M. Aida, Y. Ishihara, H. Miyahara, and A. Okino, J. Anal. At. Spectrom. (2015), doi:10.1039/C4JA00480A.
[11] T. Iwai, K. Kakegawa, K. Okumura, M. Kanamori-Kataoka, H. Miyahara, Y. Seto, and A. Okino, J. Mass Spectrom. **49**, 522 (2014).
[12] T. Takamatsu, A. Kawate, K. Uehara, T. Oshita, H. Miyahara, D. Dobrynin, G. Fridman, A. Fridman, and A. Okino, Plasma Medicine **2**, 237 (2012).
[13] S. U. Kalghatgi, G. Fridman, M. Cooper, G. Nagaraj, M. Peddinghaus, M. Balasubramanian, V. N. Vasilets, A. F. Gutsol, A. Fridman, and G. Friedman, IEEE Trans. Plasma Sci. **35**, 1559 (2007).
[14] G. Fridman, M. Peddinghaus, H. Ayan, A. Fridman, M. Balasubramanian, A. Gutsol, A. Brooks, and G. Friedman, Plasma Chem. Plasma Process **26**, 425 (2006).
[15] J. Heinlin, G. Morfill, M. Landthaler, W. Stolz, G. Isbary, J. L. Zimmermann, T. Shimizu, and S. Karrer, J. Dtsch. Dermatol. Ges. **8**, 968 (2010).
[16] G. Lloyd, G. Friedman, S. Jafri, G. Schultz, A. Fridman, and K. Harding, Plasma Process. Polym. **7**, 194 (2010).
[17] S. Iseki, K. Nakamura, M. Hayashi, H. Tanaka, H. Kondo, H. Kajiyama, H. Kano, F. Kikkawa, and M. Hori, Appl. Phys. Lett. **100**, 113702 (2012).
[18] M. Vandamme, E. Robert, S. Lerondel, V. Sarron, D. Ries, S. Dozias, J. Sobilo, D. Gosset, C. Kieda, B. Legrain, J. M. Pouvesle, and A. L. Pape, Int. J. Cancer **130**, 2185 (2012).
[19] D.T. Pham and R.S. Gault, Int. J. Machine Tools & Manufacture **38**, 1257 (1998).
[20] G. E. Ryan, A. S. Pandit, and D. P. Apatsidis, Biomaterials **29**, 3625 (2008).
[21] K. V. Wong and A. Hernandez, ISRN Mechanical Engineering **2012**, 208760 (2012).
[22] R. S. Mason, P. D. Miller, and I. P. Mortimer, Phys. Rev. E **55**, 7462 (1997).
[23] E. Karakas, M. Koklu, and M. Laroussi, J. Phys. D **43**, 155202 (2010).
[24] J. T. Herron and D. S. Green, Plasma Chem. Plasma Proc. **21**, 459 (2001).
[25] D. X. Liu, M. Z. Rong, X. H Wang, F. Iza, M. G. Kong, and P. Bruggeman, Plasma Process. Polym. **7**, 846 (2010).
[26] D. X. Liu, P. Bruggeman, F. Iza, M. Z. Rong, and M. G. Kong, Plasma Sources Sci. Technol. **19**, 025018 (2010).
[27] B. Surowsky, O. Schlüter, and D. Knorr, Food Eng Rev (2014), doi: 10.1007/s12393-014-9088-5.
[28] M. Kohno, M. Yamada, K. Mitsuta, Y. Mizuta, and T. Yoshikawa, Bull. Chem. Soc. Jpn. **64**, 1447 (1991).
[29] T. Takamatsu, K. Uehara, Y. Sasaki, H. Miyahara, Y. Matsumura, A. Iwasawa, N. Ito, T. Azuma, M. Kohno, and A. Okino, RSC Adv. **4**, 39901 (2014).
[30] T. Oshita, H. Kawano, T. Takamatsu, H. Miyahara, and A. Okino, IEEE Trans on Plasma Sci. **43**, 1987 (2015).